[Downloaded from www.aece.ro on Saturday, October 13, 2018 at 08:40:38 (UTC) by 159.226.100.198. Redistribution subject to AECE license or copyright.]

Energy Efficient Control of High Speed IPMSM Drives - A Generalized PSO Approach

Marko GECIĆ, Mirna KAPETINA, Darko MARČETIĆ
Faculty of Technical Science, University of Novi Sad, 21000 Novi Sad, Serbia
gecicm@uns.ac.rs

***Abstract*—In this paper, a generalized particle swarm optimization (GPSO) algorithm was applied to the problems of optimal control of high speed low cost interior permanent magnet motor (IPMSM) drives. In order to minimize the total controllable electrical losses and to increase the efficiency, the optimum current vector references are calculated offline based on GPSO for the wide speed range and for different load conditions. The voltage and current limits of the drive system and the variation of stator inductances are all included in the optimization method. The stored optimal current vector references are used during the real time control and the proposed algorithm is compared with the conventional high speed control algorithm, which is mostly voltage limit based. The computer simulations and experimental results on 1 kW low cost high speed IPMSM drive are discussed in details.**

***Index Terms*—energy efficiency, field oriented control, high speed, permanent magnet synchronous motor, particle swarm optimization.**

I. INTRODUCTION

The electromechanical conversion consumes almost 60% of electric energy produced in industrialized countries. With the global trend of dealing with energy efficiency issues the losses during the electromechanical conversion cannot be ignored and have to be minimized [1]. This is one of the main reasons for wide use of energy efficient permanent magnet synchronous motor (PMSM) in many applications, such as hybrid vehicles, servo-drives, household appliances, etc. [2]. Next step in the development of PMSM control techniques leads towards the improvement of energy efficiency, which can be done by manipulating the flux reference or by increasing the rotor speed [3].

Drive losses consists of converter losses and motor losses. Motor losses are losses in stator windings, mechanical losses and iron losses. The past several years saw the development of a number of loss optimization methods for regulated PMSM drives. These methods can be divided into two basic groups: methods based on search algorithms [1-4], and model-based methods [5-16]. The first group is independent of the motor model and includes inverter losses, but may, in some cases, cause ripples in steady-state torque. The second group requires the knowledge of motor (as well as power converter) parameters.

A required property for optimization by search algorithms is constant output power. In search algorithms the input power is measured and then minimized by alteration of a chosen system variables, such as rotor flux reference, direct component of current vector, etc. Search algorithms are most often used in steady-state operation but, optionally, can be combined with model-based methods during transient states. Authors in [1] have estimated input power, based on measured currents and DC circuit voltage and used search algorithm to determine the optimal d-axis current vector component for steady-state operation. An adaptive algorithm for online interior PMSM (IPMSM) loss optimization is presented in [2]. The algorithm operates in steady-state only. The authors of [3] have presented an algorithm suitable for scalar PMSM control in battery powered electric vehicle drive. Input power is calculated by using DC current and voltage and it is minimized by regulating the inverter output voltage.

Model-based algorithms require proper modeling of both motor and power converter. In order to improve the optimization the model parameter variations can also be tracked online [5]. In [8] and [9], the authors utilize the estimated stator flux vector as an independent variable for both torque and voltage equations and propose power loss reduction through voltage angle correction. The proposed solution takes into consideration both voltage and current limits, also expressed through the stator flux vector. The selection of optimal currents is based on look-up tables, generated offline using various programs.

This paper will consider the high speed IPMSM efficiency optimization provided by generalized particle swarm optimization (GPSO) algorithm. Generalized PSO algorithm is a swarm intelligence optimization technique inspired by the nature, especially in the interactions of flocks of birds and swarms of insects [17]. Due to its simplicity in concept, the PSO has been successfully applied in solving numerous practical engineering problems. In many nonlinear systems where analytic search and linear programming cannot be applied, one can find that the PSO offers satisfactory performances for solving complicated problems. In the last decade PSO was used for numerous purposes in PMSM drives: for automatic diagnosis of stator fault [18], [19] for parameter estimation [20], and for tuning of the speed controller, [19-25].

In this paper, the proposed GPSO algorithm is used to reduce copper and iron losses, both in constant field and field weakening modes of operation. Optimal stator current vector coordinates are found offline using GPSO for different load and rotor speed values. Resulting current vector coordinates are stored in the microprocessor look-up tables for later online usage during the real time control of the motor. The performances of the proposed algorithm are compared with a conventional high speed IPMSM drive algorithm in which the d-axis current reference is provided by the outer voltage regulating loop which guarantees the

This research was funded by the Ministry of Education, Science and Technological Development of Republic of Serbia under contract No. III 042004.

Digital Object Identifier 10.4316/AECE.2016.01004

1582-7445 © 2016 AECE

[Downloaded from www.aece.ro on Saturday, October 13, 2018 at 08:40:38 (UTC) by 159.226.100.198. Redistribution subject to AECE license or copyright.]

drive operation below the voltage limit [5].

The paper is organized as follows. Section III gives basic mathematical model of IPMSM with the controllable losses included. The iron losses are modeled by a speed dependent parallel resistance. In Section IV the GPSO algorithm is presented and the GPSO based optimization of IPMSM drive losses is described step by step. PSO based scheme for optimal real-time control of high-speed IPMSM and computer simulation results are presented in Section V. The graphical presentation of offline populated 2D look-up table containing optimal dq current references is also given. The experimental results are given in Section VI.

II. List of the Used Symbols

v_d ,v_q	stator d- and q-axis input voltages
v_{od} ,v_{oq}	stator d- and q-axis input voltages
i_d, i_q	stator d- and q-axis input currents
i_{do}, i_{qo}	stator d- and q-axis airgap currents
i_{dc}, i_{qc}	stator d- and q-axis iron loss currents
R_s	stator phase resistance
R_c	iron losses resistance
Ψ_m	permanent magnet flux
L_d, L_q	stator d- and q-axis self-inductances
ρ	saliency ratio (L_q/L_d)
ω_r	mechanical angular velocity
ω	electrical angular velocity
T	torque
p	number of pole pairs
P_{Cu}	copper losses
P_{Fe}	iron losses
P_L	total electric power losses

III. IPMSM Model with Controllable Power Losses Included

Fig. 1 shows steady state d- and q-axis equivalent circuits of PMSM in the dq coordinate frame which rotates synchronously with electrical angular velocity ω [12]. The same circuit can be used for both interior PMSM (where d- and q-axis inductance are not equal, $L_d \neq L_q$) and surface PMSM ($L_d = L_q = L_s$).

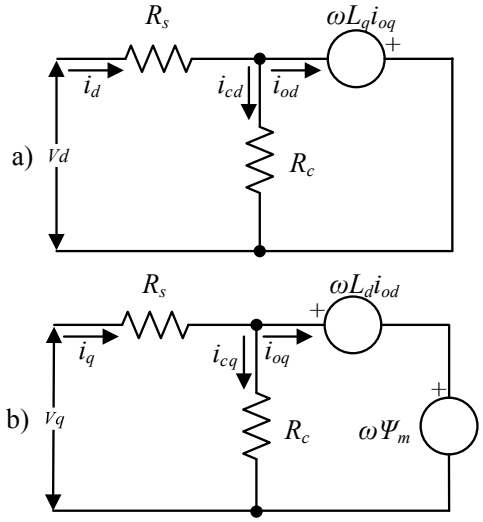


Figure 1. Equivalent circuits of PMSM: a) d-axis, b) q-axis

Based on Fig. 1 the mathematical equations of the equivalent dq axis model of IPMSM in the rotor reference frame are expressed as [7]:

$$\begin{bmatrix} v_d \\ v_q \end{bmatrix} = R_s \begin{bmatrix} i_d \\ i_q \end{bmatrix} + \left(1 + \frac{R_s}{R_c}\right) \begin{bmatrix} v_{od} \\ v_{oq} \end{bmatrix}, \tag{1}$$

$$\begin{bmatrix} v_{od} \\ v_{oq} \end{bmatrix} = \begin{bmatrix} 0 & -\omega\rho L_d \\ \omega L_d & 0 \end{bmatrix} \begin{bmatrix} i_{od} \\ i_{oq} \end{bmatrix} + \begin{bmatrix} 0 \\ \omega\psi_m \end{bmatrix}, \tag{2}$$

$$i_{od} = i_d - i_{cd}, i_{oq} = i_q - i_{cd}, \tag{3}$$

$$i_{od} = -\frac{\omega\rho L_d i_{oq}}{R_c}, i_{oq} = \frac{\omega\left(\Psi_m + L_d i_{od}\right)}{R_c}. \tag{4}$$

The iron losses, modeled by a parallel resistance R_c which is a function of rotor speed, are shown in Fig. 2. The parallel resistance is estimated via no load test with presumption that entire no-load losses are dominantly due to the iron losses [12]. The variation of the L_d and L_q inductances due to magnetic saturation effect are shown in Fig. 3 as function of stator current level.

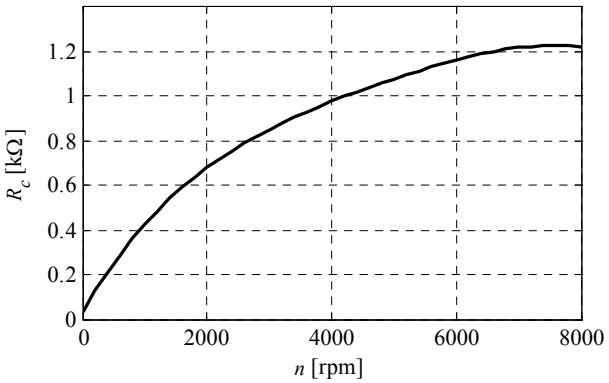


Figure 2. Parallel resistance R_c as function of speed

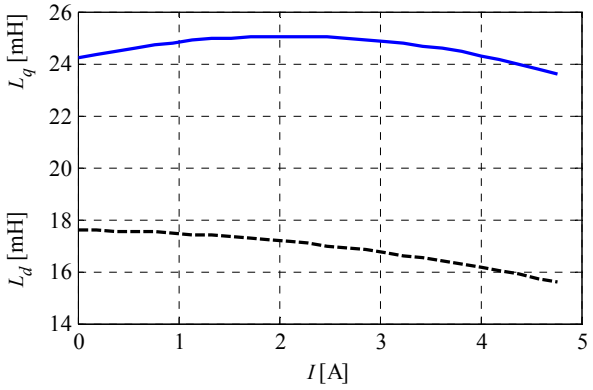


Figure 3. Inductances L_d and L_q as function of stator current

The electromagnetic torque of the IPMSM consist of two components: synchronous magnetic torque, proportional to the product of the magnet flux and q-axis stator current, and the reluctance torque, dependent on the saliency ratio and to the product of dq-axis stator current components. Based on Fig.1 the torque can be expressed as:

$$T = \frac{3}{2} p\left(\Psi_m i_{oq} + (1-\rho) L_d i_{od} i_{oq}\right). \tag{5}$$

The copper losses are proportional to square of the stator current amplitude and can be calculated using:

$$P_{Cu} = \frac{3}{2} R_s \left(i_d^2 + i_q^2\right). \tag{6}$$

The iron losses consist of two components: hysteresis and eddy current losses. The iron losses can be estimated using:

[Downloaded from www.aece.ro on Saturday, October 13, 2018 at 08:40:38 (UTC) by 159.226.100.198. Redistribution subject to AECE license or copyright.]

$$P_{Fe} = \frac{3}{2} R_c \left(i_{cd}^2 + i_{cq}^2 \right). \quad (7)$$

The mechanical losses are uncontrollable, whereas the electrical losses are controllable by current vector control. The total electrical losses consist of copper and iron losses:

$$P_L = P_{Cu} + P_{Fe}. \quad (8)$$

The controllable electrical losses can be expressed as function of i_{od}, T and ω from (3) to (7):

$$P_L = f\left(i_{od}, T, \omega\right). \quad (9)$$

Minimum of controllable electrical losses of PMSM (9) can be found by differentiating the electrical losses P_L with respect to current i_{od} and equating the derivate to zero:

$$\partial P_L / \partial i_{od} = 0. \quad (10)$$

The explicit analytical solution of (10) exists only for SPMSM [7]:

$$i_{od} = -\frac{L_d \omega^2 \psi_m \left(R_c + R_s\right)}{L_d^2 \omega^2 \left(R_c + R_s\right) + R_s R_c^2}, \quad (11)$$

while for IPMSM it cannot be found and other methods of losses optimization have to be used. Additionally, the IPMSM must operate under the voltage (V_{max}) and current (I_{max}) constrains which also have to be included in the losses optimization procedure:

$$\sqrt{i_d^2 + i_q^2} \le I_{\max}, \quad (12)$$

$$\sqrt{v_d^2 + v_q^2} \le V_{\max}. \quad (13)$$

Usually, I_{max} is 150 – 200% of rated motor current, while the V_{max} is $V_{dc} / \sqrt{3}$ when the inverter is controlled by space vector pulse with modulation in linear regime (V_{dc} is DC-link voltage amplitude). Above the rated speeds (in the field weakening range) voltage drop on stator phase resistance can be neglected and voltage limit can be expressed as:

$$\left(i_d + \frac{\psi_m}{L_d} \right)^2 + \left(\frac{L_q}{L_d} i_q \right)^2 \le \left(\frac{V_{\max}}{\omega L_d} \right)^2. \quad (14)$$

The basic idea for IPMSM control optimization lies in fact that for any speed and torque value there exists an optimal current vector that provides minimal power losses. For example, Fig. 4 shows the value of the total controllable losses as function of i_{od} for a given speed and load torque. The diagram shows the existence of such i_{od} current that can yield to minimal controllable losses.

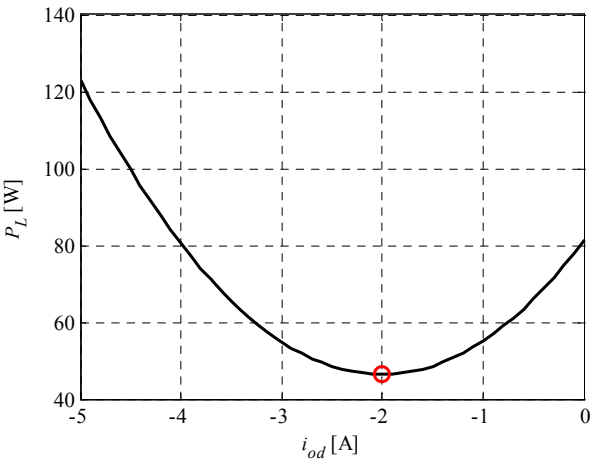


Figure 4. Total controllable electrical losses as function of d-axis airgap current at 8 krpm and 0,4 Nm

IV. Introduction to Particle Swarm Optimization

The PSO main goal is to explore the search space of interest using groups made of particles. A group of particles makes swarm, which is identified with a population in evolutionary terms. Each particle is characterized by its current position which represents a potential solution of the optimization problem and its current velocity [17].

Velocity is the difference between the current and previous positions. The initial position of each particle is randomly set within the search space, while the initial velocities are randomly chosen from the prescribed interval of allowable values. Particles compute their criterion values at each iteration, and use this information to update their position within the search space. Each particle remembers its best personal position in the history of the search that can be denoted by p_{best}, while swarm remembers the best global position within the swarm, denoted by g_{best}. In particle swarm optimization (PSO), a particle's movement is guided by two solutions, the swarm's global best and the particle's personal best. The basic idea of the PSO algorithm is that particles are moving guided by the personal and global best positions through the search space. PSO calculates a new value of velocity in every iteration. A new position of each particle is updated by the following expressions:

$$\begin{aligned} v[k+1] &= w \cdot v[k] + cp \cdot rp[k] \cdot \left(p[k] - x[k]\right) \\ &\quad + cg \cdot rg[k] \cdot \left(g[k] - x[k]\right), \end{aligned} \quad (15)$$

$$x[k+1] = x[k] + v[k+1]. \quad (16)$$

The parameters w, cp and cg represent inertial, cognitive and social component, while rp and rg are independent, uniformly distributed random numbers in the range [0, 1]. Their values are changed in order to improve performance which led to different modifications of the PSO algorithm [26-30]. Here, the Generalized PSO (GPSO) algorithm is used. GPSO is inspired by linear control theory [26],[29].

The authors in [26-30] have identified particles swarm with dynamical system of second order with two inputs and one output and then analyzed their stability. The input is represented by personal and global position of the particle, and the output of system is the current position of the particle. The position of each individual particle in GPSO is updated according to the recursive formula:

$$\begin{aligned} x[k+1] &= 2\xi\delta x[k] - \delta^2 x[k-1] + (1 - 2\xi\delta + \delta^2) \cdot \\ &\quad (c \cdot p_{best}[k] + (1-c) g_{best}[k]), \end{aligned} \quad (17)$$

where δ being the damping factor linearly decreased from 0.95 to 0.6, c being the relative cognitive factor which determines the relative influence of the personal best and the global best attractor and its value is varied from 0.8 to 0.2, ξ being the oscillation factor randomly chosen in each iteration from interval [-0.9, 0.6].

The GPSO as an optimization algorithm can work in optional n-dimensional space. The GPSO based optimization control of IPMSM drives is described as follows:

Step 1: The construction of fitness function with constrains based on current and voltage limits. The penalty function can be designed here for transforming the constraints into the fitness value function to make the model being an unconstrained optimization problem. The penalty function is the punishment for violating the constraints.

[Downloaded from www.aece.ro on Saturday, October 13, 2018 at 08:40:38 (UTC) by 159.226.100.198. Redistribution subject to AECE license or copyright.]

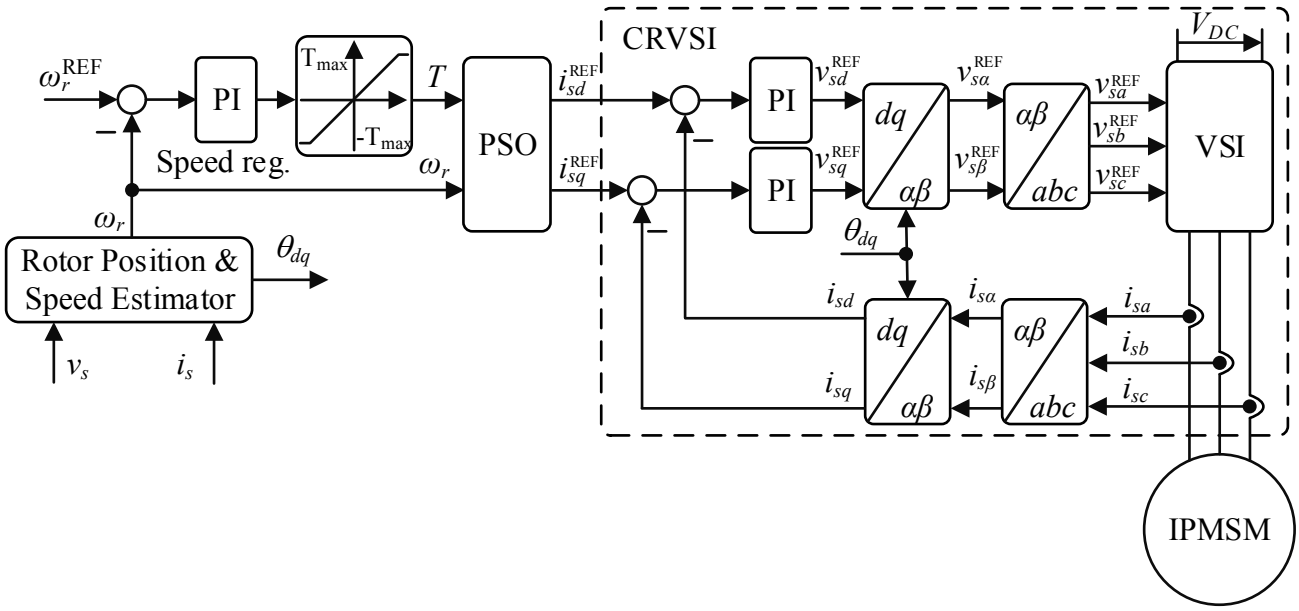


Figure 5. PSO based energy efficient interior permanent magnet synchronous motor drive

The fitness function $F(x)$ is formed by the objective function plus penalty terms for particles that have violated some inequality constraints:

$$F(x) = f(x) + \sum_{i=1}^{m} p_i \max(0, c_i(x))^2, \qquad (18)$$

where $f(x)$ is the objective function (9), $c_i(x) \le 0$ denotes constrains (12-13) and p_i denotes the penalty factor.

Step 2: During this step the number of particles (swarm size) and number of iterations are specified; the initial population is generated randomly and p_{best} are set to be the same as the initial population.

Step 3: The values of the fitness function of all particles are evaluated; p_{best} of each particle is set to current position; g_{best} is set to be initial particle with the best fitness value.

Step 4: The position and the velocity particles are updated according to (17) respectively.

Step 5: Evaluation of the updated population. For each particle, comparison of its current fitness value with the value of its p_{best} is introduced. If the current value is better than update p_{best} and g_{best} of the particle.

Step 6: Check if a stopping criterion is satisfied. If it is not satisfied, go back to Step 4. Otherwise, the optimization process is ended with the best solution g_{best} found.

V. PSO Based Scheme for Optimal Control of High Speed IPMSM

The PSO based scheme for optimal control of high-speed IPMSM is presented in the Fig 5. The only difference compared to the conventional control scheme is in PSO block which provides optimal current references for each load (T) and speed (ω_r) pair, yielding to minimum of controllable losses.

The PSO block shown in Fig 5 is practically 2D lookup table which contains optimal dq current pairs calculated offline by using GPSO optimization. During the offline table population phase the GPSO algorithm is called ones for each predicted load and speed pair, then the search for minimum power losses is performed and resulting current coordinates are stored in the table. The search predicts the motor parameter variation, such as R_c with speed and L_d and L_q with current level.

The rest of the control structure is quite common for shaft-sensorless IPMSM vector controlled drives. The rotor position and speed are estimated using terminal quantities [26] and further used for field orientation and speed control. The speed regulator block provides the torque reference which is, together with the estimated rotor speed, used as input of the PSO block. The optimal stator current references are read from PSO block and fed to the dq current regulators within the current regulated voltage source inverter (CRVSI).

The detailed flowchart of the optimal stator current references calculation algorithm for whole range of speeds and load torques is shown in Fig. 6.

The search for optimal stator current values is based on GPSO algorithm (described in Section IV) and it is performed once for each pair of torque and speed. The GPSO algorithm for one speed and torque pair considers all relevant motor parameters as constants, with the L_d and L_q values established using current reference inherited from the previous GPSO algorithm run and R_c calculated for a given speed. This simplifies the GPSO calculation process and it turns out to be justified for small torque steps in which it is not expected for current level to change drastically between two consecutive GPSO runs. Initial population for airgap d-axis current values is set for each GPSO run as random numbers in the interval (-10, 0). The number of allowed iterations used in optimization process was set to 40 and number of the particles in populations was set to 25. Once the one GPSO algorithm step is finished the (9) is used as fitness (criteria) function of optimization algorithm.

The total number of GPSO algorithm calls depends on the expected speed and torque range, as well as of the desired speed and load reference resolution which defines the step size. In the flowchart the maximum operating speed is noted as n_{max} (8000 rpm is used) and the speed step as Δn (100rpm). Also, it is recognized that the maximum torque T_{max} is the speed dependent, as shown in Fig. 7, whereas the torque step was kept constant and set to ΔT (0.01Nm).

[Downloaded from www.aece.ro on Saturday, October 13, 2018 at 08:40:38 (UTC) by 159.226.100.198. Redistribution subject to AECE license or copyright.]

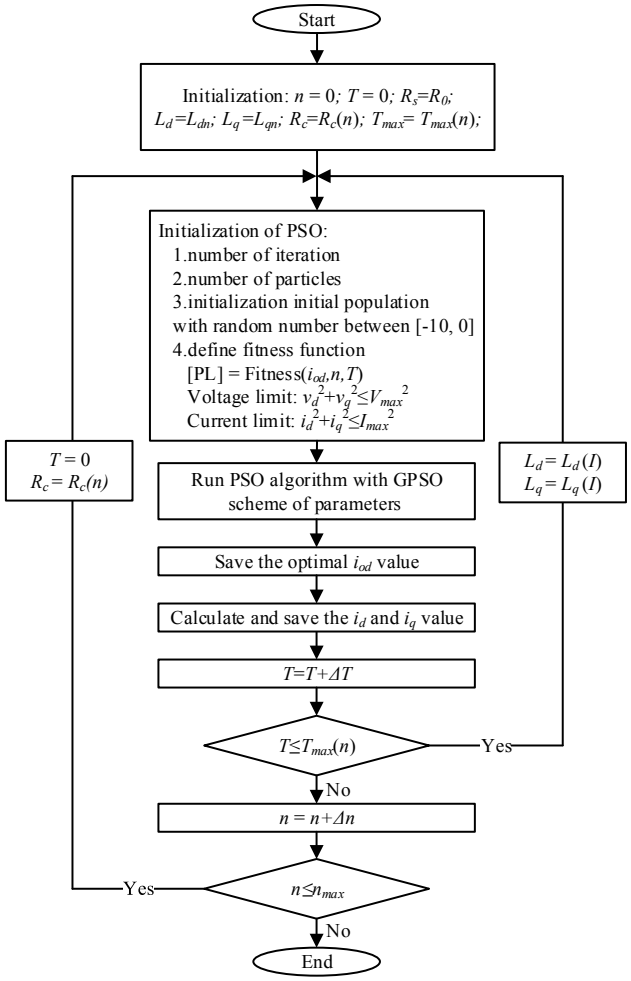


Figure 6. Flowchart of PSO optimization algorithm with the result in optimal dq current pair for each speed and load used for offline calculation of reference currents

The flowchart contains two loops. One inner loop is valid for one speed and for $T_{max}/\Delta T$ torque values. Due to the speed dependence of T_{max} the number of inner loop laps varies from 150 at constant torque range to 60 at maximum speed. The resulting stator current components from one GPSO call are used to interpolate the new values of parameters L_d and L_q which will be used for the next torque load. The flowchart also performs n_{max} / Δn outer loops in which the speed value is varied from 0 to the expected maximum value. For every new outer loop lap the speed is increased, the speed dependent parameter R_c is changed and the inner loop torque counter is reset to zero. Also, the L_d and L_q are preset to the rated values.

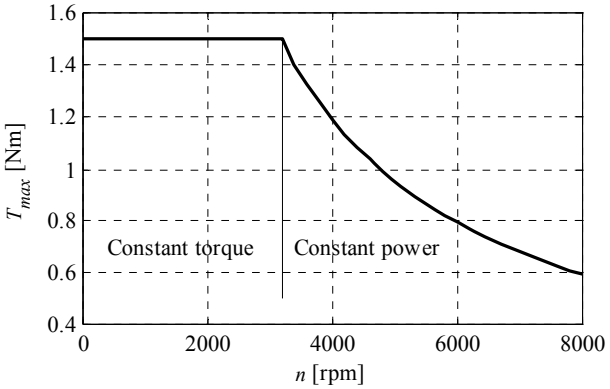


Figure 7. Maximum load torque in the constant torque and the constant output power region

Calculated optimal i_{od} current component and electrical losses for wide speed and torque are shown in Fig. 8 and Fig. 9, respectively.

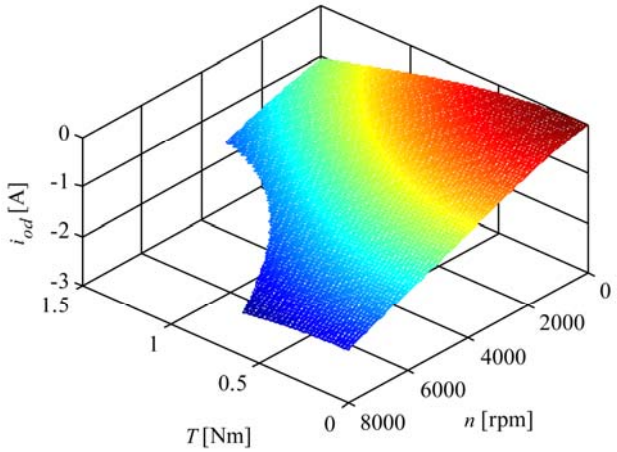


Figure 8. Optimal airgap currents for the given speed and load torque ranges

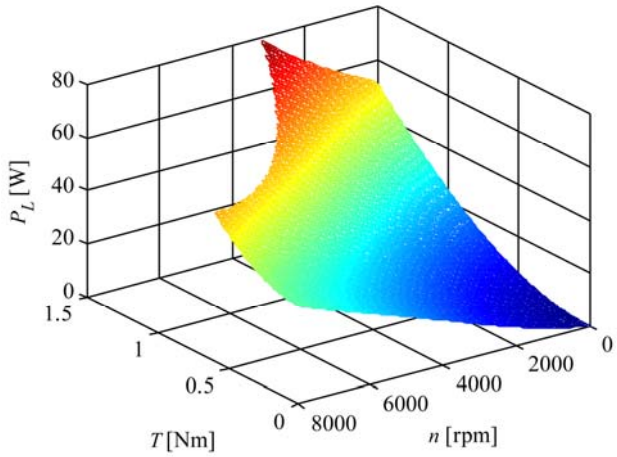


Figure 9. Minimal electrical losses for the given speed and load torque ranges

Based on optimal i_{od} current component and (3) and (4) optimal dq-axis current components are calculated and shown in Fig. 10 and in Fig. 11, respectively. Energy efficiency for the given speed and torque range is shown on Fig.12.

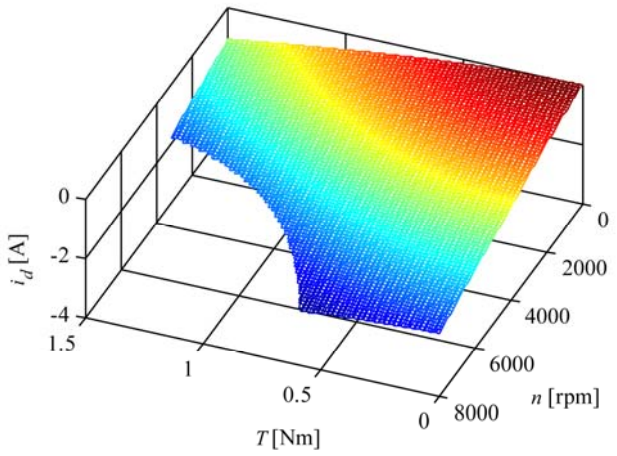


Figure 10. Optimal i_d for the given speed and load torque ranges

[Downloaded from www.aece.ro on Saturday, October 13, 2018 at 08:40:38 (UTC) by 159.226.100.198. Redistribution subject to AECE license or copyright.]

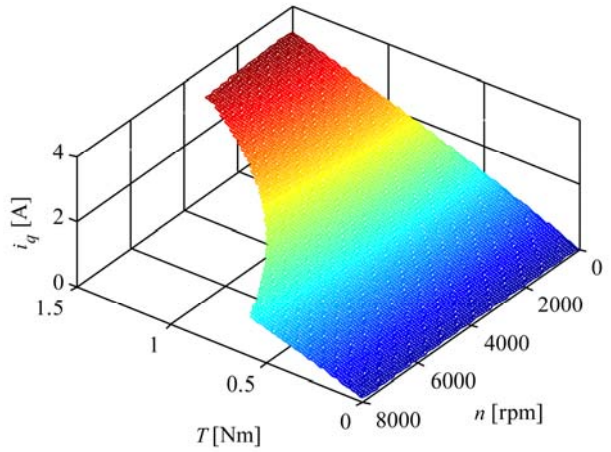


Figure 11. Optimal i_q for the given speed and load torque ranges

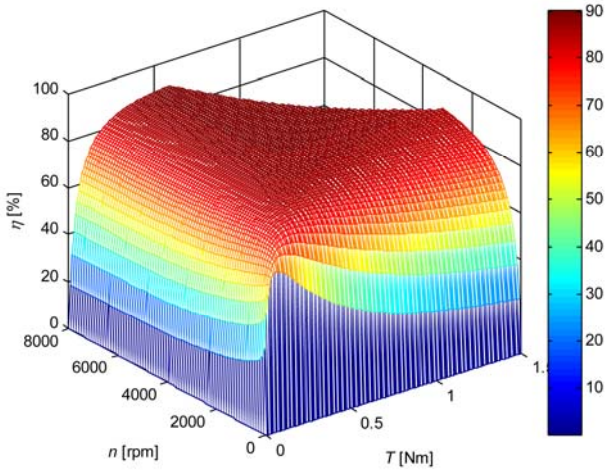


Figure 12. Energy efficiency for the given speed and load torque ranges

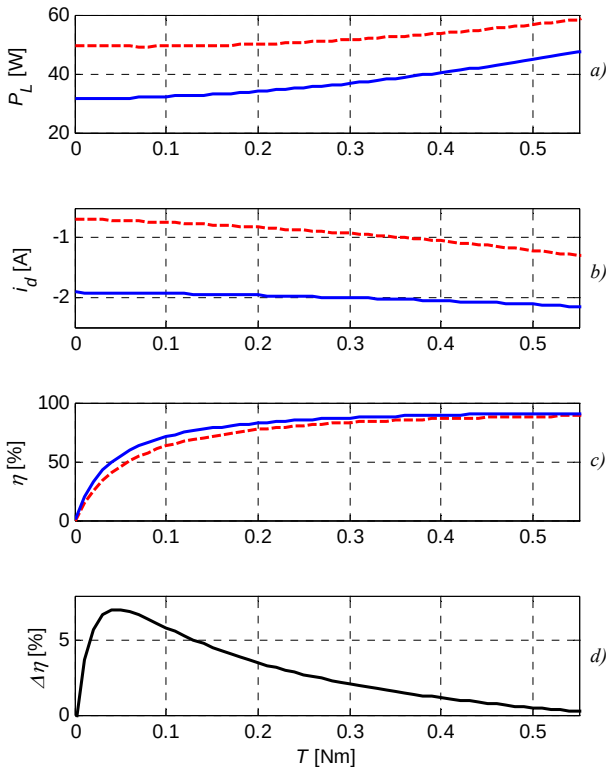


Figure 13. Simulation results: Comparison of a) losses, b) direct stator current component, c) efficiency and d) energy efficiency difference between two methods for different loads at 8 krpm

Fig. 13 shows computer simulation results for electrical losses as a function of load at given speed (8krpm). The results cover two control types: the conventional control method always operating at the voltage limit (red, dashed), and the suggested GPSO current references based control algorithm (blue, solid). One can notice that controllable losses are always lower when GPSO current references are used. In general, the negative d-axis current reference calculated by the GPSO algorithm is always higher, which results in the reduction of motor flux, and, thus, in the reduction of the iron losses. At the same time the copper losses are increased, but the total electrical controllable losses are still lower. Because of the fact that iron losses are getting progressively dominated as speed gets higher, it is obvious that GPSO algorithm yields to better efficiency in the whole high speed range of IPMSM drive.

VI. Experimental Results

The block diagram of used experimental setup is shown in Fig. 14. The experiments were performed on high speed IPMSM with its parameters listed in the Table 1. The motor was controlled by low cost 1kW vector drive based on Infineon Control Integrated Power System (CIPOS) IGCM06F60GA 600V/6A module operating at 16 kHz PWM frequency. The drive operates shaft-sensorless, and contains only one current shunt placed in the dc circuit from which the three motor phase currents are reconstructed online.

The GPSO algorithm based IPMSM drive control scheme shown on Fig. 5 is executed in real time, every PWM period on Freescale DSP 56F8245 operating at 60 MHz. The rotor position and speed estimation are performed using shaft-sensorless extended back-EMF algorithm [31].

The IPMSM is loaded with MAGTROL HD-705-7 brake. Based on maximum load torque for selected speed, as shown in Fig. 7, several points of interest are tested. The data from DSP were transferred in real time into the PC via fast serial interface and plotted in Matlab.

TABLE I. Parameters of the IPMSM

Parameter	Value
R_s (Ω)	3.04
L_d (mH)	16.64
L_q (mH)	24.99
Ψ_m (Wb)	0.07
P (W)	1000
p	4

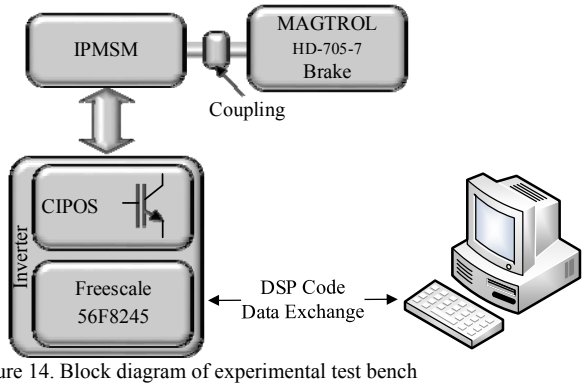


Figure 14. Block diagram of experimental test bench

[Downloaded from www.aece.ro on Saturday, October 13, 2018 at 08:40:38 (UTC) by 159.226.100.198. Redistribution subject to AECE license or copyright.]

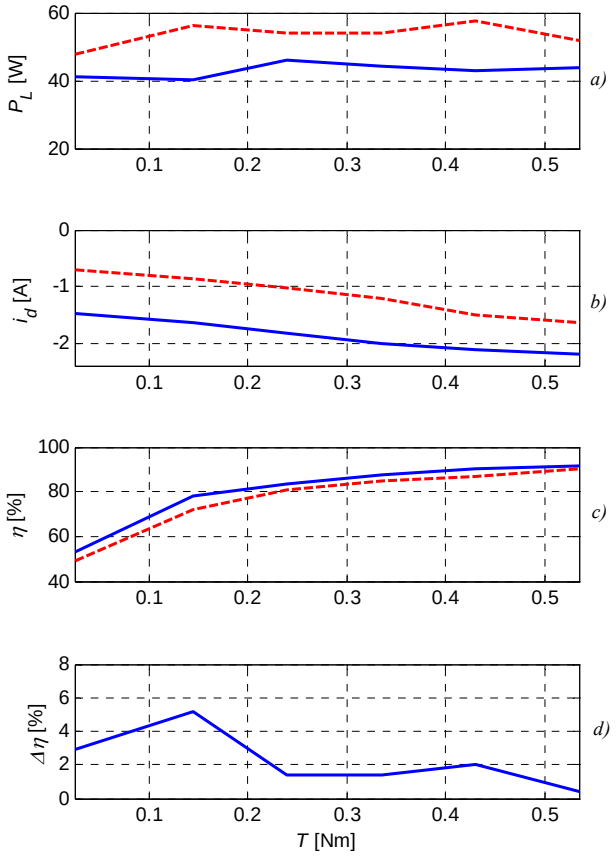


Figure 15. Experimental results: Comparison of a) losses, b) direct stator current component, c) efficiency and d) energy efficiency difference between two methods for different loads at 8 krpm

Fig. 15 shows experimental results for electrical losses as a function of load at given speed (8krpm is selected) for the two control types: the conventional type with voltage limit (red, dashed), and the GPSO algorithm based control (blue, solid). The results were collected for several load points, up to 0.55 Nm at given speed. There are small differences between tracks in Fig.13 and Fig. 15 due to non-modeled friction losses. One can notice that in each load point the GPSO algorithm yields to the better efficiency. Improvement is more significant at light loads in same cases up to 6%.

VII. Conclusion

In this paper the lookup table based approach for optimal control of high speed IPMSM drives has been presented. The lookup table is populated offline with GPSO based power losses minimization algorithm results for each expected pair of speed and torque. The optimal stator current reference calculation algorithm is further improved with the motor parameter variation prediction between two successive algorithm calls. The whole expected speed and torque range are covered using multiple GPSO calls, with predefined speed and torque steps. Once generated offline, the lookup table results are easy used as speed and reference torque dependent current references in the existing IPMSM real time control algorithm. The experiments show that this approach results in significant reduction of power losses, compared with conventional high speed IPMSM drive operating at voltage limit. The proposed method can be extended to induction motor drive system by changing mathematical model and optimization criteria.

References

[1] Z. Q. Zhu and L. M. Gong, "Improved sensorless operation of permanent magnet brushless AC motors based on online optimal efficiency control," in Electric Machines Drives Conference (IEMDC), 2011 IEEE International, 2011, pp. 1591–1596. doi:10.1109/IEMDC.2011.5994598

[2] S. Vaez, V. I. John, and M. A. Rahman, "An on-line loss minimization controller for interior permanent magnet motor drives," IEEE Transactions on Energy Conversion, vol. 14, no. 4, pp. 1435–1440, Dec. 1999. doi:10.1109/60.815086

[3] C. C. Chan and K. T. Chau, "An advanced permanent magnet motor drive system for battery-powered electric vehicles," IEEE Transactions on Vehicular Technology, vol. 45, no. 1, pp. 180–188, Feb. 1996. doi:10.1109/25.481836

[4] A. R. A. Taheri, "Energy Optimization of Field Oriented Six-Phase Induction Motor Drive," Advances in Electrical and Computer Engineering, vol. 11, no. 2, pp. 107–112, 2011. doi:10.4316/aece.2011.02017

[5] J.-M. Kim and S.-K. Sul, "Speed control of interior permanent magnet synchronous motor drive for the flux weakening operation," IEEE Transactions on Industry Applications, vol. 33, no. 1, pp. 43–48, Jan. 1997. doi:10.1109/28.567075

[6] R. Bojoi, M. Pastorelli, J. Bottomley, P. Giangrande, and C. Gerada, "Sensorless control of PM motor drives - A technology status review," in 2013 IEEE Workshop on Electrical Machines Design Control and Diagnosis (WEMDCD), 2013, pp. 168–182. doi:10.1109/WEMDCD.2013.6525177

[7] S. Morimoto, Y. Tong, Y. Takeda, and T. Hirasa, "Loss minimization control of permanent magnet synchronous motor drives," IEEE Transactions on Industrial Electronics, vol. 41, no. 5, pp. 511–517, Oct. 1994. doi:10.1109/41.315269

[8] S.-Y. Jung, J. Hong, and K. Nam, "Copper loss minimizing torque control of IPMSM based on flux variables," in Electric Machines Drives Conference (IEMDC), 2013 IEEE International, 2013, pp. 1174–1179. doi:10.1109/IEMDC.2013.6556282

[9] B. Patel and M. N. Uddin, "Development of a nonlinear loss minimization control of an IPMSM drive with flux estimation," in Electric Machines Drives Conference (IEMDC), 2013 IEEE International, 2013, pp. 1196–1203. doi:10.1109/IEMDC.2013.6556285

[10] H. Aorith, J. Wang, and P. Lazari, "A new Loss Minimization Algorithm for Interior Permanent Magnet Synchronous Machine drives," in Electric Machines Drives Conference (IEMDC), 2013 IEEE International, 2013, pp. 526–533. doi:10.1109/IEMDC.2013.6556146

[11] H.-C. Chen, K.-Y. Chen, and W.-Y. Chen, "High-Efficiency Current Control Methods Based on Multidimensional Feedback Quantization and Its Application to Three-Phase PMSM," IEEE Transactions on Industrial Electronics, vol. 61, no. 11, pp. 5820–5829, Nov. 2014. doi:10.1109/TIE.2014.2316230

[12] A. Rabiei, T. Thiringer, and J. Lindberg, "Maximizing the energy efficiency of a PMSM for vehicular applications using an iron loss accounting optimization based on nonlinear programming," in 2012 XXth International Conference on Electrical Machines (ICEM), 2012, pp. 1001–1007. doi:10.1109/ICElMach.2012.6349998

[13] R. Ni, D. Xu, G. Wang, L. Ding, G. Zhang, and L. Qu, "Maximum Efficiency Per Ampere Control of Permanent-Magnet Synchronous Machines," IEEE Transactions on Industrial Electronics, vol. 62, no. 4, pp. 2135–2143, Apr. 2015. doi:10.1109/TIE.2014.2354238

[14] I. Vlad, A. Campeanu, S. Enache, and G. Petropol, "Operation Characteristics Optimization of Low Power Three-Phase Asynchronous Motors," Advances in Electrical and Computer Engineering, vol. 14, no. 1, pp. 87–92, 2014. doi:10.4316/AECE.2014.01014

[15] M. Leuer, A. Ruting, and J. Bocker, "Efficiency-optimized Model Predictive Torque Control for IPMSM, " in Energy Conference (ENERGYCON), 2014 IEEE International , vol., no., pp.9-13, 13-16 May 2014. doi:10.1109/ENERGYCON.2014.6850398

[16] Y. Zhang, K. Yang, H. Xie, C. Zhu, X. Wei, and Z. Pan, "Optimal efficiency control of modular PMSM on EVs based on iso efficiency contours, " in Electrical Machines and Systems (ICEMS), 2014 17th International Conference on , vol., no., pp.2131-2135, 22-25 Oct. 2014. doi:10.1109/ICEMS.2014.7013837

[Downloaded from www.aece.ro on Saturday, October 13, 2018 at 08:40:38 (UTC) by 159.226.100.198. Redistribution subject to AECE license or copyright.]

[17] J. Kennedy and R. Eberhart, "Particle swarm optimization," in , IEEE International Conference on Neural Networks, 1995. Proceedings, 1995, vol. 4, pp. 1942–1948 vol.4. doi:10.1109/ICNN.1995.488968

[18] L. Liu and D. A. Cartes, "A particle swarm optimization approach for automatic diagnosis of PMSM stator fault," in American Control Conference, 2006, p. 6, doi:10.1109/ACC.2006.1657181

[19] F. Grouz, L. Sbita, and M. Boussak, "Particle swarm optimization based fault diagnosis for non-salient PMSM with multi-phase inter-turn short circuit," in 2012 2nd International Conference on Communications, Computing and Control Applications (CCCA), 2012, pp. 1–6. doi:10.1109/CCCA.2012.6417873

[20] Z.-H. Liu, J. Zhang, X.-H. Li, and Y.-J. Zhang, "Cooperative particle swarm optimization with ICS and Its application to parameter identification of PMSM," in 2012 7th IEEE Conference on Industrial Electronics and Applications (ICIEA), 2012, pp. 1303–1308. doi:10.1109/ICIEA.2012.6360923

[21] S. Yan, D. Xu, X. Gui, and M. Yang, "On-line Particle Swarm Optimization of Anti-Windup Speed Controller for PMSM Drive System," in 2nd IEEE Conference on Industrial Electronics and Applications, 2007. ICIEA 2007, 2007, pp. 278–282. doi:10.1109/ICIEA.2007.4318415

[22] H. Hu, Q. Hu, Z. Lu, and D. Xu, "Optimal PID controller design in PMSM servo system via particle swarm optimization," in 31st Annual Conference of IEEE Industrial Electronics Society, 2005. IECON 2005, doi:10.1109/IECON.2005.1568882

[23] H. Aygun, M. Gokdag, M. Aktas, and M. Cernat, "A novel sensorless field oriented controller for Permanent Magnet Synchronous Motors, " in Industrial Electronics (ISIE), 2014 IEEE 23rd International Symposium on, pp.715-720, 1-4 June 2014. doi:10.1109/ISIE.2014.6864700

[24] M. Baskin, and B. Caglar, "A modified design of PID controller for permanent magnet synchronous motor drives using particle swarm optimization, " in Power Electronics and Motion Control Conference and Exposition (PEMC), 2014 16th International , vol., no., pp.388-393, 21-24 Sept. 2014. doi:10.1109/EPEPEMC.2014.6980524

[25] Z. Q. Song, D. Xiao, and M.F. Rahman, "Online particle swarm optimization for sensorless IPMSM drives considering parameter variation, " in Power Electronics Conference (IPEC-Hiroshima 2014 - ECCE-ASIA), 2014 International , vol., no., pp.2686-2692, 18-21 May 2014. doi:10.1109/IPEC.2014.6869970

[26] A. Ratnaweera, S. Halgamuge, and H. C. Watson, "Self-organizing hierarchical particle swarm optimizer with time-varying acceleration coefficients," IEEE Transactions on Evolutionary Computation, vol. 8, no. 3, pp. 240–255, Jun. 2004. doi:10.1109/TEVC.2004.826071

[27] M. R. Rapaic, Z. Kanovic, Z. D. Jelicic, and D. Petrovacki, "Generalized PSO algorithm - an application to Lorenz system identification by means of neural-networks," in 9th Symposium on Neural Network Applications in Electrical Engineering, 2008. NEUREL 2008, pp. 31–35. doi:10.1109/NEUREL.2008.4685554

[28] M. R. Rapaić and Ž. Kanović, "Time-varying PSO – convergence analysis, convergence-related parameterization and new parameter adjustment schemes," Information Processing Letters, vol. 109, no. 11, pp. 548–552, May 2009. doi:10.1016/j.ipl.2009.01.021

[29] Ž. Kanović, M. R. Rapaić, and Z. D. Jeličić, "Generalized particle swarm optimization algorithm - Theoretical and empirical analysis with application in fault detection," Applied Mathematics and Computation, vol. 217, no. 24, pp. 10175–10186, Aug. 2011. doi:10.1016/j.amc.2011.05.013

[30] O. T. Altinoz, A. E. Yilmaz, A. Duca, G. Ciuprina, "Incorporating the Avoidance Behavior to the Standard Particle Swarm Optimization 2011," Advances in Electrical and Computer Engineering, vol.15, no.2, pp.51-58, 2015, doi: 10.4316/AECE.2015.02007

[31] D. Yousfi and A. Darkawi, "Comparison of two position and speed estimation techniques used in PMSM sensorless vector control," in 4th IET Conference on Power Electronics, Machines and Drives, 2008. PEMD 2008, 2008, pp. 626–630.